International Journal of Computational and Experimental Science and ENgineering (IJCESEN)

Vol. 11-No.2 (2025) pp. 2423-2435
http://www.ijcesen.com

ISSN: 2149-9144

Research Article

Anthropogenic and Climate Change Impacts on Diwaniya River Water Quality

Saraa M. Ali [1,*] , Mohammed S. Shamkhi[2,3], Zaid Abed Al-Ridah[4]

[1]Al-Qasim Green University, Water Resources Management Engineering Department, College of Engineering, Babylon, 51013, Iraq
* **Corresponding Author Email:**saraa.m213017@wrec.uoqasim.edu.iq -- **ORCID:** 0009-0007-2960-1626

[2]Department of Structures and Water Resources, Faculty of Engin., University of Kufa, Najaf AlAshraf, Iraq
[3]College of Engineering, University of Warith Al-Anbiyaa, Karbala, Iraq
Email: mohammeds.alfahdy@uokufa.edu.iq -- **ORCID:** 0000-0002-3591-7404

[4]Civil Engineering Department, College of Engineering, Al-Qasim Green University, Babylon 51013, Iraq
Email: zaidalmnsory@wrec.uoqasim.edu.iq -- **ORCID:** 0000-0002-4311-9760

Article Info:

DOI: 10.22399/ijcesen.1537
Received : 18 January 2025
Accepted : 23 March 2025

Keywords :

HEC-RAS 5.0.5,
Euphrates River,
Al-Diwaniya River,
Mathematical Modelling.

Abstract:

This study aims investigates the calibration and validation of the HEC-RAS model to simulate critical water quality parameters in Iraq's semi-arid environment, focusing on its application for sustainable water resource management. Using a robust dataset of observed and simulated values, the research examined biochemical oxygen demand (BOD_5), total dissolved solids (TDS), dissolved oxygen (DO), electrical conductivity (EC), nitrate (NO_3^-), phosphate (PO_4^{3-}), calcium (Ca), and magnesium (Mg). The calibration and validation results demonstrated strong alignment between observed and simulated data, with high R^2 values for key parameters such as NO_3^- ($R^2 = 0.94$ for validation) and PO_4^{3-} ($R^2 = 0.96$ for calibration), affirming the model's reliability in predicting nutrient dynamics. The study identified variations in model accuracy, with TDS exhibiting percentage errors ranging from 1.70% to 8.73% and challenges in simulating DO, where negative errors exceeded 12%. These discrepancies reflect the complexity of modeling organic matter decomposition and oxygen dynamics under fluctuating climatic and flow conditions. Additionally, pollution hotspots characterized by elevated EC and TDS levels were detected, underscoring the significant impact of anthropogenic activities on water quality. By providing a validated framework for simulating critical water quality indicators, this study contributes to water quality modeling in arid and semi-arid regions. The findings offer valuable insights for policymakers, emphasizing the integration of advanced hydrological models with sustainable management practices. This research advocates for adaptive strategies to mitigate water quality degradation, addressing challenges posed by climate change and increasing population pressures.

1. Introduction

The increasing degradation of water quality due to anthropogenic pressures such as industrialization, urbanization, and agricultural runoff has become a critical environmental concern worldwide. Rivers, as dynamic freshwater systems, are particularly vulnerable to pollution, which adversely affects their ecological balance, compromises aquatic biodiversity, and endangers human health. In response to these challenges, the development and application of advanced hydrodynamic models have emerged as indispensable tools for understanding, predicting, and managing water quality in river systems. Among these, the Hydrologic Engineering Center's River Analysis System (HEC-RAS) stands out as a sophisticated, one-dimensional modeling framework that facilitates the simulation of river hydraulics, pollutant transport, and water quality dynamics [1]. This study focuses on applying the HEC-RAS model to simulate water quality in the Al-Diwaniya River, Iraq, a river that serves as a vital resource for agriculture, industry, and domestic use. Over the years, this river has faced escalating challenges due to the discharge of untreated wastewater, agricultural runoff enriched with fertilizers, and effluents from industrial activities [2]. These factors have resulted in the accumulation of pollutants, including nutrients such as phosphorus, and deteriorated the overall water quality, posing serious risks to public health and the surrounding ecosystems. Despite its critical importance, there is a noticeable lack of comprehensive studies utilizing advanced hydrodynamic models like HEC-RAS to address water quality issues in the Iraqi riverine context. This study, therefore, represents a pioneering effort to simulate the transport and fate of key pollutants in the Al-Diwaniya River, with a focus on understanding its flow characteristics and longitudinal water quality distribution [3]. Water quality models such as HEC-RAS play a pivotal role in integrating hydrodynamic and water quality data to analyze the spatiotemporal distribution of pollutants under diverse flow regimes. These models are invaluable for establishing water quality standards, formulating pollution control strategies, and predicting the environmental impacts of different management interventions. The HEC-RAS model, developed by the U.S. Army Corps of Engineers, is particularly renowned for its capability to simulate steady and unsteady flow conditions, as well as its detailed representation of hydraulic structures such as weirs and sluices. This model has been extensively applied worldwide to assess flood risks, simulate pollutant dispersion, and evaluate water quality under complex scenarios. However, its application in simulating pollutant transport and evaluating water quality parameters in rivers within arid and semi-arid regions, such as Iraq, remains underexplored. In this research, the HEC-RAS model is utilized to simulate the hydraulic and environmental characteristics of the Al-Diwaniya River, with a focus on key water quality parameters, including biochemical oxygen demand (BOD), dissolved oxygen (DO), total phosphorus (TP), electrical conductivity (EC), and total dissolved solids (TDS). The study provides a detailed analysis of the longitudinal distribution of these parameters under varying flow conditions, offering insights into the interactions between hydrodynamic processes and pollutant transport. Such an approach is essential for identifying critical pollution hotspots, understanding nutrient dynamics, and assessing the potential impacts of anthropogenic activities on water quality [4]. The motivation for this research stems from the critical role of water as a cornerstone of life and its indispensable contribution to agricultural productivity, industrial activities, and domestic consumption. The degradation of water quality not only threatens public health through the proliferation of waterborne diseases but also disrupts ecological functions, leading to the loss of aquatic biodiversity and productivity. This underscores the urgent need for scientifically robust and regionally adapted water quality models that can guide policymakers and stakeholders in developing sustainable management strategies [5]. Through the application of the HEC-RAS model, this study aims to bridge the knowledge gap regarding the dynamics of water quality in the Al-Diwaniya River. By simulating the interaction between hydrodynamics and pollutant transport, this research not only advances the understanding of water quality dynamics but also underscores the importance of integrating modeling approaches in the sustainable management of riverine ecosystems. The outcomes are anticipated to serve as a foundation for designing effective mitigation strategies to improve water quality, thereby contributing to the preservation of water resources in Iraq and other regions facing similar environmental challenges [6].

2. Research setting

The study focuses on the Al-Diwaniya River, located within the Al-Diwaniya Governorate in Iraq. This river serves as a vital water resource for the region, supporting multiple uses such as irrigation, domestic consumption, and other community needs. Originating in the northern city of Sadr Al-Dughra, the river extends approximately 120 kilometers before reaching the Al-Muthanna Governorate, traversing key communities including Al-Diwaniya, Al-Sidair, and Al-Hamzah[7]. This research specifically examines an 8-kilometer segment of the river within the densely populated urban area of Al-Diwaniya city. The high population density and the river's critical role in meeting municipal and agricultural water demands underscore the importance of assessing its water quality. Monitoring and analysis of this stretch are crucial for understanding the impact of anthropogenic activities and guiding the development of effective water management strategies. The geographical scope of the study is illustrated in (Figure 1), providing an overview of the river's path and the targeted study area.

3. Model description

3.1 Data Collection and Sources

The data pertaining to water quality were gathered from multiple credible and authoritative sources, including the Ministry of Water Resources and the Ministry of Environment in Iraq. Additionally, insights were drawn from previous studies and

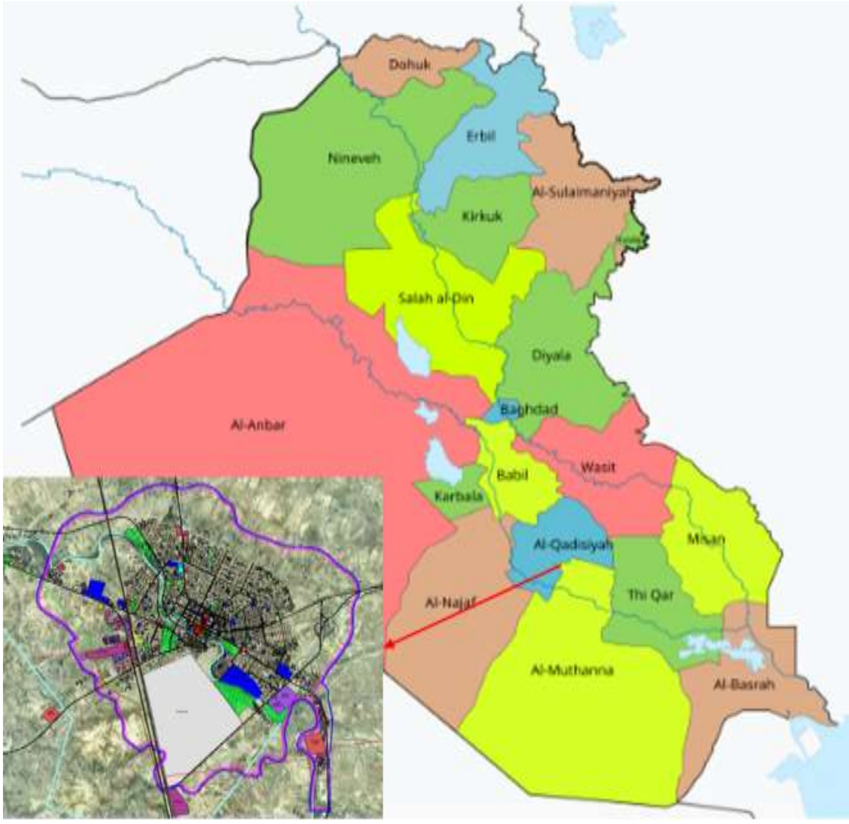

***Figure 1**. Map showing the study area along Al-Diwaniyah.*

research focusing on water quality in the Euphrates and Al-Diwaniyah Rivers. Hydrological and geological data were acquired from relevant governmental agencies and esteemed scientific institutions to ensure the reliability and comprehensiveness of the information [8]. The water quality data were specifically sourced from monitoring stations located within the Al-Diwaniyah Marsh area, enabling accurate and detailed assessments. This meticulous approach ensures that the dataset is robust and suitable for drawing valid inferences regarding water quality in the study area. The integration of diverse data sources strengthens the foundation of the research, supporting the precise evaluation and simulation of water quality parameters within the Al-Diwaniyah River system [9].

3.2 Pre-processing of Data

Data processing is a pivotal stage that precedes the initiation of water quality modeling using the HEC-RAS model. Sampling and data collection were conducted at pre- and post-pollution discharge points, as well as at intervals between these locations along the river [10]. This approach ensured comprehensive coverage of the study area and provided essential insights into the spatial distribution of pollutants. The collected data underwent thorough examination to ensure accuracy and reliability, which are critical for the efficacy of the modeling process. Specialized software tools were utilized to verify and process the data, converting it into a format compatible with the HEC-RAS model. This conversion facilitated seamless input and efficient use of the data in the modeling and simulation process [11]. Water samples were collected from 14 designated locations, carefully selected to provide a representative analysis of the river's water quality. These samples were analyzed for various water quality parameters, including pH, Electrical Conductivity (EC), Dissolved Oxygen (DO), Total Suspended Solids (TSS), Biochemical Oxygen Demand (BOD), phosphate, temperature, and nutrient concentrations. The results from these tests formed the basis for simulating water quality within the HEC-RAS framework, enabling a detailed understanding of the river's pollution dynamics and informing effective management strategies [12].

4. Water Quality Parameters and Monitoring Stations

The critical water quality parameters identified for monitoring in the study area include pH, dissolved oxygen (DO), biochemical oxygen demand (BOD), total suspended solids (TSS), electrical conductivity (EC), hardness, chlorides, alkalinity, phosphate, calcium, magnesium, and total dissolved solids

(TDS). Monitoring stations have been strategically established along the Al-Diwaniyah River to measure these parameters accurately [13]. The selection of these stations was based on key factors, such as areas prone to pollution and the river's flow dynamics. Data collected from these stations will provide precise and reliable insights into the water quality, serving as the foundation for analysis and simulation using the HEC-RAS model [14].

4.1 Reaeration Rate and Dispersion Coefficient

The reaeration rate and dispersion coefficient have been estimated using equation (1), (2), (3) respectively. For the Umhlangane River the average velocity is 0.67m/s and depth is 2.942 m. According to Bowie et al. (1985), the coefficient (Kr) in modeling is extremely sensitive and crucial for forecasting other water quality parameters. The re-aeration coefficient can be computed using a variety of semi-empirical equations. One of these is the assumption that the re-aeration coefficient depends on temperature and hydraulic parameters, specifically depth and velocity [14].

In rivers, a number of variables have an effect on the estimation of the longitudinal dispersion coefficient. The most essential ones are: the viscosity, channel width, flow depth, density, shear velocity, mean velocity, bed slope, horizontal stream curvature, and bed shape factor and bed roughness [15].

$$E_{p,i} 0.011 \, \frac{{U_i}^2 B^2}{U_i^* H_i} \qquad (\mathbf{1})$$

If $\frac{W}{H} \leq 30.6 \; then \; D_L = 15.49$

$$\left(\frac{W}{H}\right)^{0.78} \left(\frac{u}{U_*}\right)^{0.11} H U_* \qquad (\mathbf{2})$$

If $\frac{W}{H} \geq 30.6 \; then \; D_L = 14.12$

$$\left(\frac{W}{H}\right)^{0.61} \left(\frac{u}{U_*}\right)^{0.85} H U_* \qquad (\mathbf{3})$$

$$E_z = K.d.u^* \qquad (4)$$

Three equations (1), (3), (4) were used, and the results Percentage Errors were calculated for each equation 0.7199, 0.086, 0.259 respectively [16].

4.2 Calibration and Validation of HEC-RAS Model

Upon completing the implementation of the HEC-RAS model and integrating the collected data, the calibration and validation processes were undertaken to ensure the model's reliability and accuracy [17]. Calibration involved adjusting the model's parameters and variables to minimize discrepancies between simulated outputs and observed field data. This iterative process ensured alignment between the theoretical results generated by the model and the actual readings obtained from the study area. Following calibration, the model was validated using an independent dataset that was not employed during the calibration phase. This step was essential to verify the model's predictive capability for environmental and hydrological variables under various conditions [18].

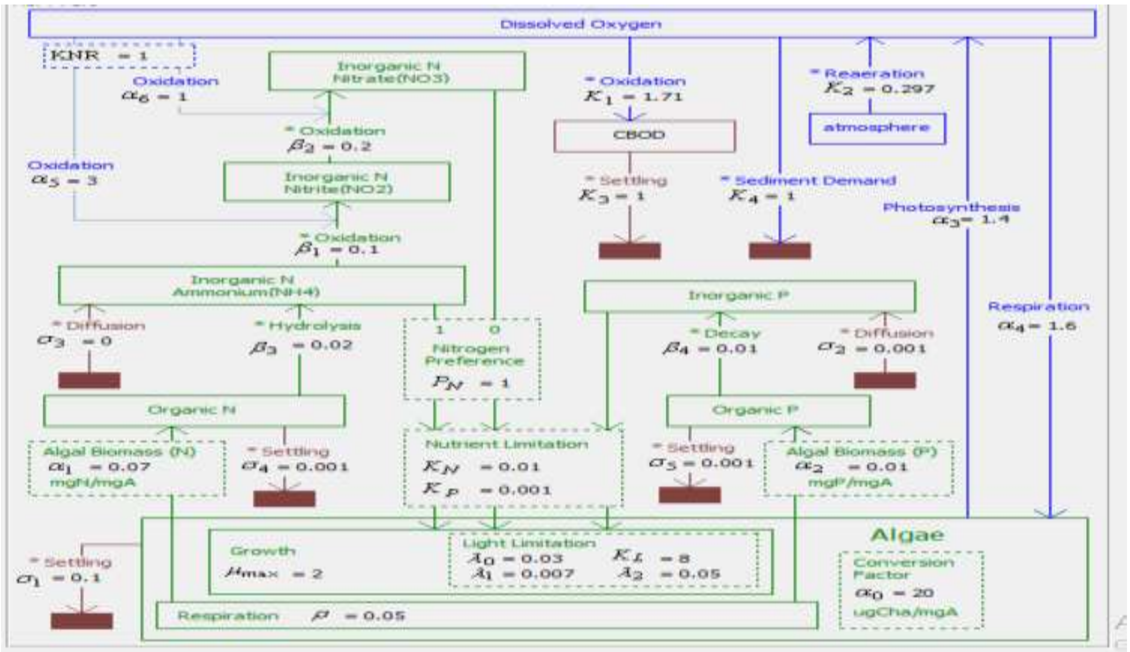

***Figure 2**. Calibration Parameters constants (HEC – RAS 5.0.5)*

By comparing simulated outcomes with real-world measurements, the validation process confirmed the model's robustness and its ability to accurately simulate water quality dynamics within the Al-Diwaniyah River system. This comprehensive approach ensures the reliability of the HEC-RAS model for future water quality assessments and management initiatives (Figure 2).

5. Results and evaluation

5.1 Calibration and Validation

Unsteady Flow

The calibration of the hydraulic model was conducted by adjusting Manning's roughness coefficients these coefficients were the primary parameters used to achieve an accurate representation of flow conditions within the study area [19]. The initial values for Manning's roughness coefficients were obtained from the Basic River Plan for the Diwaniya River, providing reliable baseline data for model adjustment. Using HEC-RAS, the average Manning's coefficient (n) was calculated for an 8 km stretch of the Al-Diwaniya River. The evaluation involved testing ten different n values, ranging from 0.016 to 0.024 (Table 1). Through the calibration process, it was determined that a value of n=0.022 provided the best balance between the observed and predicted water levels, ensuring a reliable representation of the river's hydraulic behavior [19]. The unsteady flow simulation was performed using observational hydraulic data, including flow rates and water levels, which were applied as boundary conditions in the HEC-RAS model. Following the calibration and validation processes Equations(5)–(6) show R^2, Percentage Error [20].

$$\boldsymbol{R^2} = \left[\frac{\sum_{i=1}^{N}(O_i-\bar{O})(S_i-\bar{S})}{\sqrt{\sum_{i=1}^{N}(O_i-\bar{O})^2}\sqrt{\sum_{i=1}^{N}(S_i-\bar{S})^2}}\right]^2 \qquad (5)$$

$$\textbf{Percentage Error (\%)} = \frac{\sum_{i=1}^{N}(O_i-S_i)}{\sum_{i=1}^{N}O_i} \times 100 \qquad (6)$$

We simulated the water quality parameters by applying these model parameters. Table2 shows the mean values of both the observational data and the simulation results for the water quality parameters from 2024(calibration) to 2023 (validation).

Comparing simulated and observed data for eight water quality parameters during the calibration across 34 and 11 cross sections

- ✓ **DO (Dissolved Oxygen) Parameter (Figure 3,4a):**

• **Observation vs. Simulation:** If the simulated DO levels align closely with observed data, this suggests the model's accuracy in predicting oxygen dynamics in the water column. Discrepancies might indicate the need for further refinement in terms of biological oxygen demand

Table 1. *Statistical indices for Calibration and Validation Results of Water Quality Parameters Using HEC-RAS for cross sections 34 and 11.*

Parameter	Calibration				Validation			
	R^2		Percentage Error (%)		R^2		Percentage Error (%)	
	34	11	34	11	34	11	34	11
BOD_5 (mg/L)	0.542	0.859	0.249	11.243	0.788	0.915	19.164	6.022
TDS (mg/L)	0.934	0.958	1.695	8.728	0.965	0.901	11.469	9.773
DO (mg/L)	0.510	0.530	-12.446	-12.587	0.947	0.777	-15.475	-12.269
EC (µS/cm)	0.810	0.762	1.596	5.320	0.645	0.480	3.798	16.026
NO_3^- (mg/L)	0.935	0.847	-18.919	1.752	0.946	0.855	-2.186	-9.668
PO_4^{3-} (mg/L)	0.958	0.963	-6.662	3.257	0.991	0.812	0.309	-2.185
Ca (mg/L)	0.868	0.790	-1.766	3.423	0.813	0.724	-3.525	1.433
Ma (mg/L)	0.714	0.828	1.747	7.194	0.944	0.930	-4.741	5.574

Table 2.*Mean values of both the observational data and the simulation results for the parameters from 2024 (calibration) and 2023 (validation).*

Parameter		**Calibration**		**Validation**	
		Cross Section			
		34	**11**	**34**	**11**
BOD_5 (mg/L)	Observational	2.197	2.127	1.965	2.671
	Simulation	1.846	1.893	1.577	2.490
TDS (mg/L)	observational	820.143	892.000	1038.786	1111.786
	Simulation	804.671	799.513	914.509	987.960
DO (mg/L)	Observational	6.716	6.447	6.313	7.002
	Simulation	8.030	8.255	7.112	5.679
EC (µS/cm)	Observational	1220.429	1259.200	1161.657	1346.729
	Simulation	1192.525	1191.930	1108.968	1109.016
NO_3^- (mg/L)	Observational	5.027	6.269	2.451	2.421
	Simulation	6.490	6.290	2.459	2.461
PO_4^{3-} (mg/L)	Observational	0.013	0.019	0.007	0.002
	Simulation	0.013	0.017	0.007	0.002
Ca (mg/L)	Observational	114.586	120.814	100.201	105.737
	Simulation	115.950	116.003	103.546	104.374
Mg (mg/L)	Observational	40.446	42.900	39.785	38.251
	Simulation	39.785	39.424	40.446	39.943

(BOD) inputs or oxygen production rates in the system [20].

- **Interpretation:** A high difference could be linked to model assumptions that do not fully capture local conditions affecting DO levels, such as temperature or microbial activity [21].

✓ **DS (Total Dissolved Solids) Parameter (Figure 3,4b):**

- **Observation vs. Simulation:** Variations between observed and simulated TDS could indicate errors in the model's representation of solute transport or water flow dynamics. For instance, [22] if TDS is consistently higher or lower in the observations, it may suggest issues with water quality inputs or the model's handling of particulate versus dissolved matter [23].
- **Interpretation:** The deviation could also arise from misrepresented interactions between water chemistry and solid material accumulation [24].

✓ **EC (Electrical Conductivity) Parameter (Figure 3,4c):**

- Observation vs. Simulation: EC levels directly relate to ion concentrations in the water. Any deviation could highlight discrepancies in ion-specific dynamics or errors in the model's conductivity equation, which may not fully capture ionic strength variations [25].
- **Interpretation:** Persistent differences between simulated and observed EC may suggest that certain solute species or environmental factors (such as temperature) were not properly accounted for in the simulation [26].

✓ **NO3 (Nitrate) Parameter (Figure 3,4d):**

- **Observation vs. Simulation:** Nitrate concentrations often fluctuate based on both biological processes (e.g., nitrification) and physical processes (e.g., dilution). A large gap between the observed and simulated NO3 could indicate either a lack of accurate input data (such as nitrogen loading) or errors in representing the cycling processes [27].
- **Interpretation:** The model's handling of nutrient uptake by plants or the role of microbial processes (e.g., denitrification) may require further adjustments [28].

✓ **PO4 (Phosphate) Parameter (Figure 3,4e):**

- **Observation vs. Simulation:** The simulation of phosphate might show either an underestimation or overestimation, which could be a result of incorrect assumptions about adsorption/desorption rates or sediment interactions [29].
- Interpretation: If the discrepancy is significant, revisiting the calibration of phosphate

removal mechanisms, such as plant uptake or microbial processes, may be necessary [30].

✓ **Ca (Calcium) Parameter (Figure 3,4f):**

• **Observation vs. Simulation:** Calcium concentrations are important in the precipitation and interaction of other ions in the water. Discrepancies between observed and simulated data might point to issues with the model's ability to simulate ion exchange or mineral precipitation accurately [31].

• **Interpretation:** Differences in calcium levels could suggest that calcium cycling, particularly in relation to carbonate precipitation, needs to be more thoroughly represented [32].

✓ **BOD5 (Biochemical Oxygen Demand for 5 days) Parameter (Figure 3,4g):**

• **Observation vs. Simulation:** If BOD5 is overestimated or underestimated, this could indicate that the microbial community dynamics or organic matter decomposition rate in the model are not accurate, leading to incorrect predictions of oxygen demand [33].

• **Interpretation:** Variability could also stem from inaccuracies in the representation of organic matter inputs or biodegradation rates under specific environmental conditions [34].

✓ **Mg (Magnesium) Parameter (Figure 3,4h):**

• **Observation vs. Simulation:** Magnesium behaves similarly to calcium in many systems, and any discrepancies could be due to model shortcomings in predicting the complex interactions between magnesium and other ions [35].

• **Interpretation:** Larger differences might suggest that magnesium dynamics, especially in the context of water hardness or ion exchange, need to be calibrated more accurately [36].

5.3. Comparing simulated and observed data for eight water quality parameters during the validation across 34 and 11 cross sections

(a) Dissolved Oxygen (DO):

The simulated values closely follow the observed trends, demonstrating a gradual decrease over time.

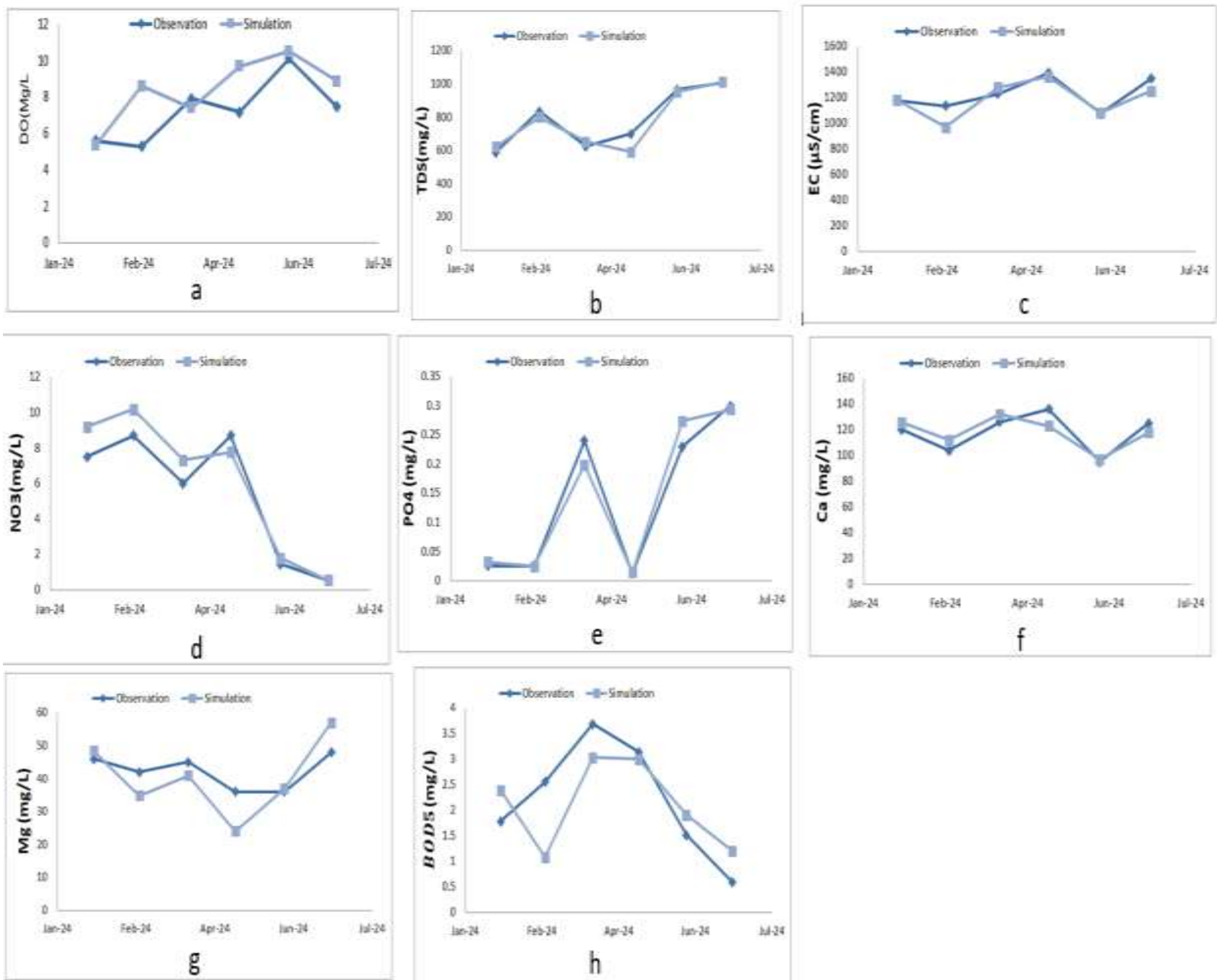

__Figure 3.__ Hydrographs showing the difference between simulation and observation for calibtionin 34 gross section. (a) Do parameter; (b) TDS parameter; (c) Ec parameter; (d) No3 parameter. (e) Po4 parameter; (f) Ca parameter; (g) BOD5 parameter; (h) Mg parameter.

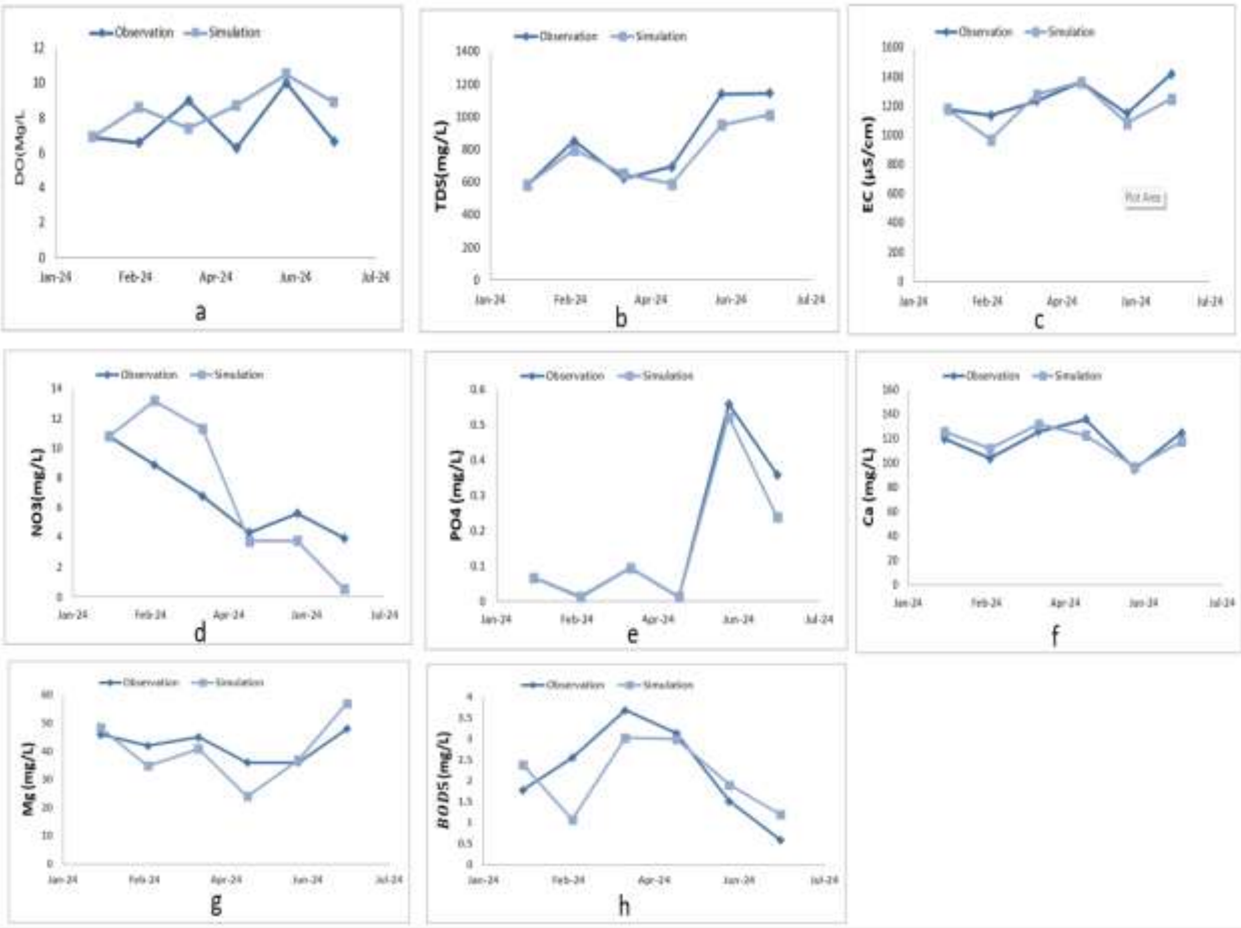

Figure 4. *Hydrographs showing the difference between simulation and observation for calibtionin 11 gross section. (a) Do parameter; (b) TDS parameter; (c) Ec parameter; (d) No3 parameter. (e) Po4 parameter; (f) Ca parameter; (g) BOD5 parameter; (h) Mg parameter.*

However (Figure 5,6), slight deviations are evident in the later months, suggesting minor model limitations in accurately capturing oxygen dynamics under varying flow conditions [37].

(b) Total Dissolved Solids (TDS):

The hydrograph indicates a strong alignment between simulated and observed data, particularly in the early and middle months (Figure 5, 6). The model successfully predicts the increasing TDS concentrations toward the later period, reflecting its reliability in simulating dissolved solids under changing hydrological scenarios [38].

(c) Electrical Conductivity (EC):

While the simulation generally aligns with observed values, noticeable discrepancies occur during the low-conductivity period in March. This may be attributed to the model's sensitivity to localized flow conditions or external influences not accounted for in the dataset [39].

(d) Nitrate (NO_3^-):

The model exhibits a high degree of accuracy in predicting nitrate concentrations throughout the validation period. Both observed and simulated values show a consistent decline, underscoring the robustness of the model in simulating nutrient transport [40].

(e) Phosphate (PO_4^{3-}):

Although the model effectively captures the decreasing trend in phosphate levels, a significant deviation is observed in the early months, potentially due to variations in external phosphate inputs or retention processes not fully represented in the model[41].

(f) Calcium (Ca):

The hydrograph reveals a strong agreement between simulated and observed values, with only minor deviations during the mid-period. This indicates the model's reliability in representing calcium dynamics under unsteady flow conditions [42].

(g) Biochemical Oxygen Demand (BOD_5):

The simulated and observed BOD_5 values demonstrate a close correlation, particularly in the later months, with a steady increase in concentration. This suggests the model accurately represents organic matter decomposition and oxygen demand processes [43].

(h) Magnesium (Mg):

The simulation effectively captures the observed trends in magnesium concentrations, with minor variations during specific periods. The alignment underscores the model's capacity to simulate magnesium transport under varying hydrological conditions (Figure 5, 6) [44].

5.4. Variations of water quality parameters along the system for calibration and validation

(a) Dissolved Oxygen (DO):
The schematic plot reveals a consistent decrease in DO levels moving downstream, indicating oxygen consumption due to organic matter degradation and microbial activity. Higher DO values upstream suggest minimal pollution sources at the initial sections [45].

(b) Total Dissolved Solids (TDS):
TDS levels exhibit an increasing trend downstream, reflecting the accumulation of dissolved ions from anthropogenic activities and natural mineral dissolution. This pattern highlights potential pollution hotspots along the flow path (Figure 7,8) [45].

(c) Electrical Conductivity (EC):
EC follows a similar pattern to TDS, with a gradual increase downstream, confirming the accumulation of ionic constituents and their proportional relationship with dissolved solids(Figure 7,8) [43].

(d) Nitrate (NO_3^-):
The nitrate distribution shows varying concentrations, with elevated levels in specific sections. These spikes could indicate localized agricultural runoff or effluent discharge containing nitrogen compounds [44].

(e) Phosphate (PO_4^{3-}):
The phosphate schematic plot demonstrates distinct areas with higher concentrations, reflecting inputs from agricultural fertilizers or untreated wastewater. Downstream reduction may indicate phosphate uptake by aquatic plants or sediment adsorption (Figure 7, 8) [42].

(f) Calcium (Ca):
Calcium concentrations display a relatively stable distribution, with minor increases downstream. This stability suggests its source is predominantly natural, such as rock weathering or groundwater contributions [44].

(g) Biochemical Oxygen Demand (BOD_5):
The schematic highlights areas with higher BOD_5 concentrations, indicating zones of significant organic pollution and microbial activity requiring oxygen for decomposition (Figure 7, 8) [45].

(h) Magnesium (Mg):
Magnesium distribution is relatively uniform, with a slight increase downstream, likely due to geochemical contributions and the dissolution of magnesium-bearing minerals(Figure 7,8) [46]. Mathematical Modelling is applied for different fields in the literature [47-57].

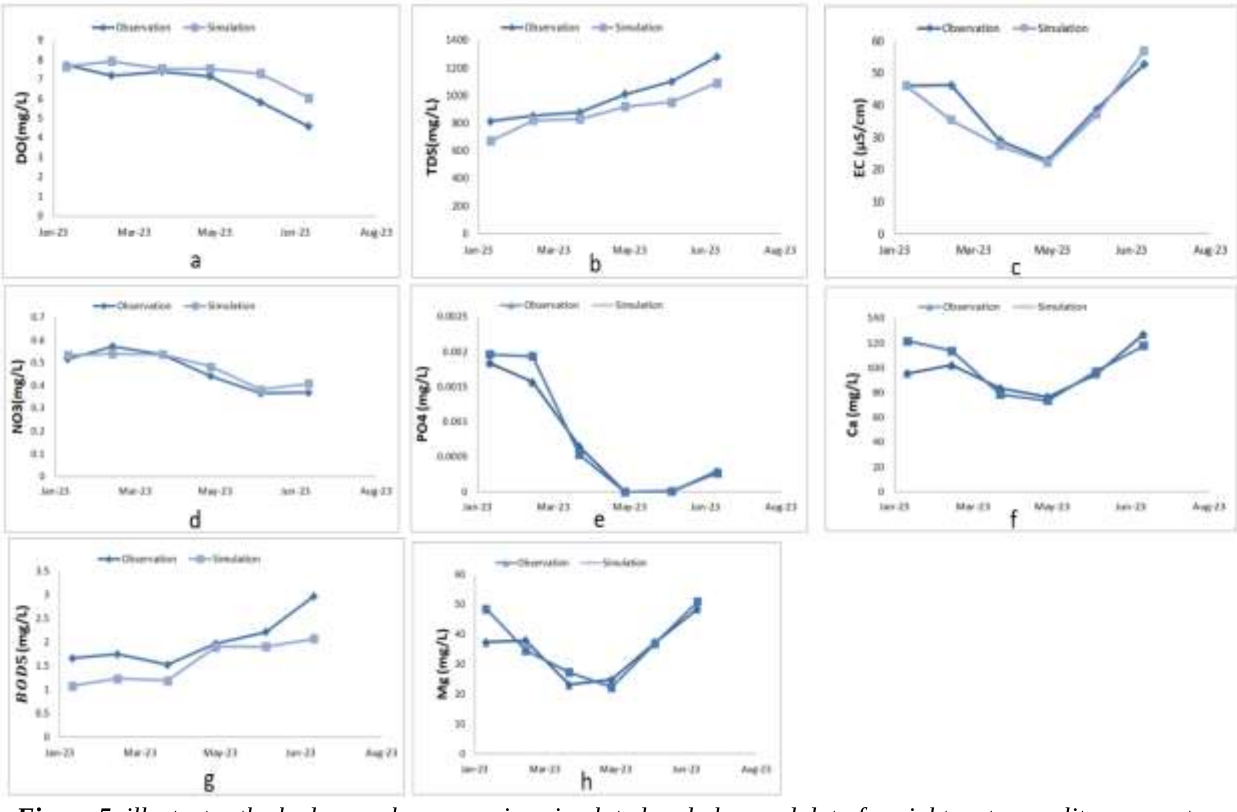

***Figure 5**. illustrates the hydrographs comparing simulated and observed data for eight water quality parameters during the validation process across 34 cross sections.*

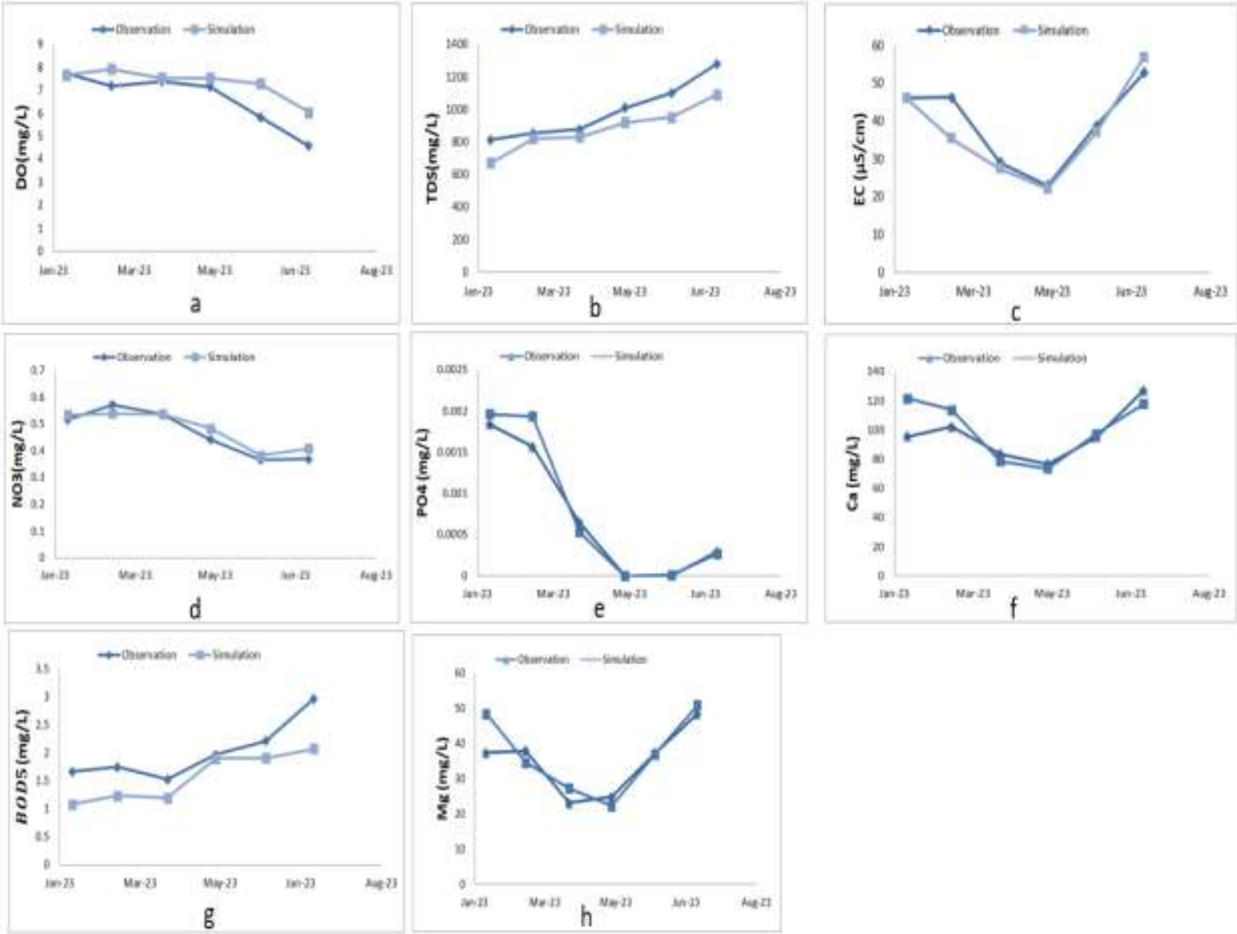

Figure 6. *compares simulated and observed data for eight water quality parameters across 11 gross sections, highlighting the model's performance during the validation phase.*

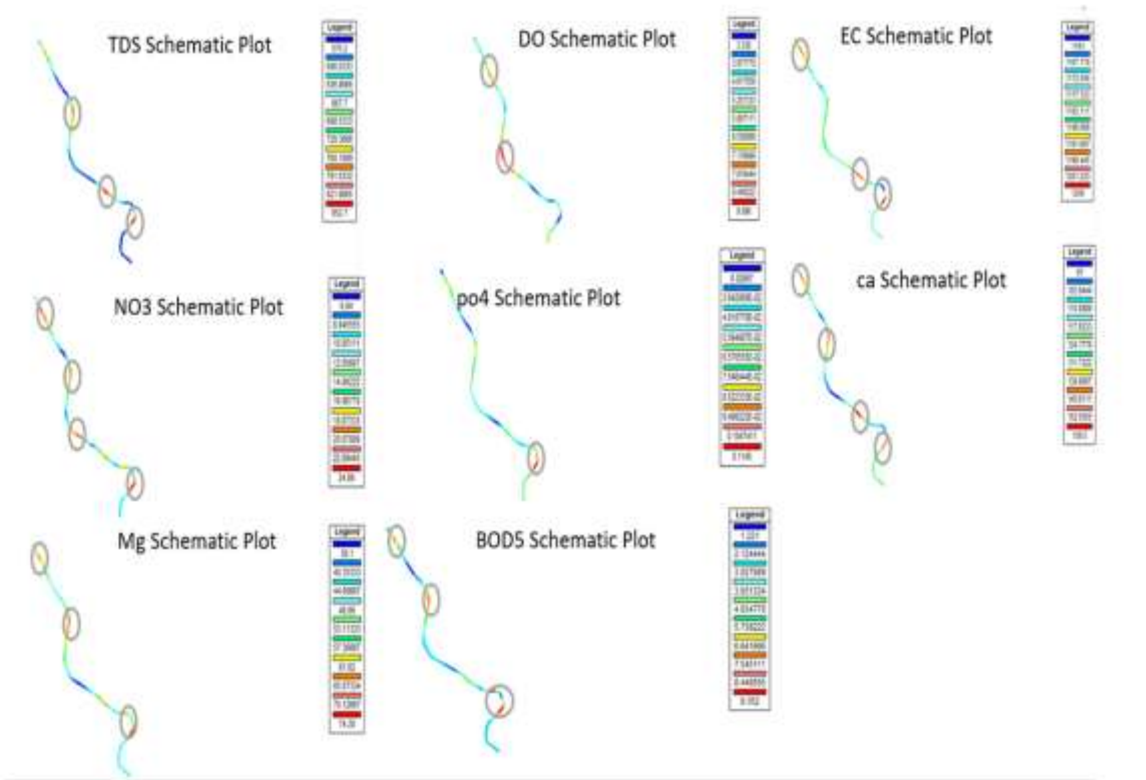

Figure 7. *illustrates the calibtionin in (a) Do parameter; (b) TDS parameter; (c) Ec parameter; (d) No3 parameter. (e) Po4 parameter; (f) Ca parameter; (g) BOD5 parameter; (h) Mg parameter.*

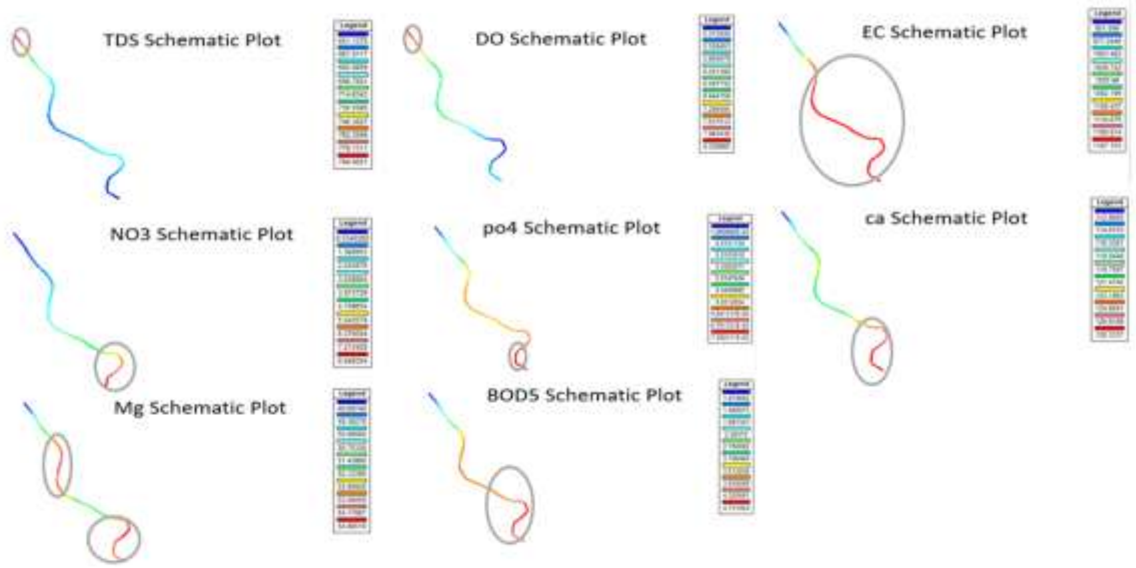

Figure 8. *illustrates the variations in (a) Do parameter; (b) TDS parameter; (c) Ec parameter; (d) No3 parameter. (e) Po4 parameter; (f) Ca parameter; (g) BOD5 parameter; (h) Mg parameter.*

Author Statements:

- **Ethical approval:** The conducted research is not related to either human or animal use.
- **Conflict of interest:** The authors declare that they have no known competing financial interests or personal relationships that could have appeared to influence the work reported in this paper
- **Acknowledgement:** The authors extend their thanks to the Iraqi Ministry for Water Resources (IMWR) and the Directorate of Water Resources in the Diwaniyah Region for providing me with the bathymetric map and flow information, which would have prohibited me to constructing a model.
- **Author contributions:** The authors declare that they have equal right on this paper.
- **Funding information:** The authors declare that there is no funding to be acknowledged.
- **Data availability statement:** The data that support the findings of this study are available on request from the corresponding author. The data are not publicly available due to privacy or ethical restrictions.

References

[1] Nenny., Hamzah, Al, Imran. (2019). Sediment Rentention Models Right On The Irrigation Channels. 50-53. doi: 10.2991/ICMEME-18.2019.12

[2] Chenoweth, J., (2008). A re-assessment of indicators of national water scarcity. *Water International*, 33(1): p. 5-18

[3] Kamel, A., (2008). Application of a hydrodynamic MIKE 11 model for the Euphrates River in Iraq. *Slovak Journal of Civil Engineering*, 2(1);1-7

[4] Hughes, D., (2019). Facing a future water resources management crisis in sub-Saharan Africa. *Journal of Hydrology: Regional Studies*, 23;100600

[5] Gil, Y., et al., (2021) Artificial intelligence for modeling complex systems: taming the complexity of expert models to improve decision making. *ACM Transactions on Interactive Intelligent Systems*, 11(2);1-49

[6] Yaseen, Z.M., et al., (2019). An enhanced extreme learning machine model for river flow forecasting: State-of-the-art, practical applications in water resource engineering area and future research direction. *Journal of Hydrology*, 569: p. 387-408

[7] Kafle, M.R. and N.M. Shakya, (2018). Two-Dimensional Hydrodynamic Modelling of Koshi River and Prediction of Inundation Parameters. *Hydrology: Current Research*. 9: p. 30

[8] Iris, Holzer. (2023). Using 2D HEC-RAS Modeling with Vertical Feature Extraction to Inform Ecological Design in the Lower Atchafalaya River Basin, Louisiana. doi: 10.31390/gradschool_theses.5655

[9] Budianto, Ontowirjo., Imam, Fathurrahman., M., Zahra., Hendra, Wahyudi. (2023). LiDAR DEM and HEC-RAS On-Grid Rainfall Hydrograph Model for Irrigation System. *IOP conference series*, 1198(1):012023-012023. doi: 10.1088/1755-1315/1198/1/012023

[10] Nadia, Nazhat, Sabeeh., Waleed, M., Sh., Alabdraba. (2022). The Hydrodynamic Model using HEC-RAS: The case of Tigris River Downstream of Samarra Barrage (Iraq). *IOP conference series*, 1120(1):012017-012017. doi: 10.1088/1755-1315/1120/1/012017

[11] D. V. Kalaba, I. B.Ivanović, D. Čikara and G. O. Milentijević,. (2014) The initial analysis of the river Ibar temperature downstream of the lake Gazivode. *Thermal science* 18, 73-80.

[12] Mohammed, J., Mawat., Ahmed, Naseh, Ahmed, Hamdan. (2023). Integration of numerical models to simulate 2D hydrodynamic/water quality model of contaminant concentration in Shatt Al-Arab River with WRDB calibration tools. *Open Engineering*, 13(1) doi: 10.1515/eng-2022-0416

[13] Shamkhi, M. S., Hafudh, A., Qa.is, H. and Amer, R., (2019) Froude number data analysis and its implications on local scour. Proceedings - *International Conference on Developments in eSystems Engineering, DeSE*, October-(2019), pp. 315–320, 9073025

[14] Shan-e-hyder, Soomro., Caihong, Hu., Muhammad, Munir, Babar., Mairaj, Hyder, Alias, Aamir. (2021). Estimation of Manning's Roughness Coefficient Through Calibration Using HEC-RAS Model: A Case Study of Rohri Canal, *Pakistan. American Journal of Civil Engineering*, 9(1):1-. doi: 10.11648/J.AJCE.20210901.11

[15] Shamkhi, M. S. and Abbasi R. T., (2024). Streamflow simulation using the integrated water resources management model on the lower basin of the Diyala river, Iraq. *AIP Conf. Proc.* 3091, 020014 https://doi.org/10.1063/5.0205417

[16] Shamkhi, M. S., Hafudh, A., Qa.is, H. and Amer, R., (2019) Froude number data analysis and its implications on local scour. Proceedings - International *Conference on Developments in eSystems Engineering, DeSE*, 2019, October-, pp. 315–320, 9073025

[17] Shamkhi, M.S., Azeez, J.M.R. and Abdul-Sahib, A.A., (2020) Morphologic and engineering characteristics of watersheds (a case study: East wasit watersheds that feed the al-Shewicha Trough - Iraq). *IOP Conference Series: Materials Science and Engineering*, 870(1), 012115

[18] Mohammed S. Shamkhi, Marwaa K. Azeez, Rawaa J. Tuama; Evaluation of the rain water network in wasit governorate/Kut city and the commercial center of the region as a dual network (rain and sewage*). AIP Conf. Proc.* 26 July 2023; 2775 (1): 070001. https://doi.org/10.1063/5.0140848

[19] Al-Zubaidi, H. A. M., Naje, A. S., Al-Ridah, Z. A., Chelliapan, S., & Sopian, K. (2024). *Numerical Modeling of Reaeration Coefficient for Lakes: A Case Study of Sawa Lake, Iraq*. https://doi.org/10.12912/27197050/185312

[20] Ahmed, A. M., & Kareem, S. L. (2024). Evaluating the role of hydraulic retention time (HRT) in pollutant removal efficiency using Arundo donax in vertical subsurface flow constructed wetlands. *Bioremediation Journal*, 1-15.

[21] S.M. Hocaoglu, (2017)Resources, conservation and recycling evaluations of on-site wastewater reuse alternatives for hotels through water balance, *Resour. Conserv. Recycl.* 122;43–50.

[22] M. Muduli, V. Sonpal, S. Ray, S. Haldar, (2022) In-depth performance study of an innovative decentralized multistage constructed wetland system treating real institutional wastewater, *Environ. Res.* 210;112896.

[23] Shamkhi M. S. and Auad M. H., (2023). Improvement of Hydraulic Characteristics for Dujila Canal. *AIP Conference Proceedings* 2977(122) https://doi.org/10.1063/5.0182187

[24] L. Liu, J. Cao, M. Ali, J. Zhang, Z. Wang (2021), Impact of green roof plant species on domestic wastewater treatment, *Environ. Adv.* 4;100059.

[25] Alfatlawi, T. J. M., & Alsultani, R. A. A. (2019). Characterization of chloride penetration in hydraulic concrete structures exposed to different heads of seawater: Using hydraulic pressure tank. *Engineering Science and Technology, an International Journal*, 22(3), 939-946.

[26] Shamkhi, M.S., Tuama, R.J. and Azeez, M.K., (2023) Experimental and 3D Numerical Simulations of Flow Over a Rounded Edge-Broad Crested Weir. *AIP Conference Proceedings*, 2806(1), 040035. https://doi.org/10.1063/5.0166656

[27] A.C. del _Alamo, M.I. Pariente, R. Molina, F. Martínez, (2022) Advanced bio-oxidation of fungal mixed cultures immobilized on rotating biological contactors for the removal of pharmaceutical micropollutants in a real hospital wastewater, *J. Hazard Mater.* 425;128002.

[28] Shamkhi, M. S. and Abbasi R. T., (2024) Streamflow simulation using the integrated water resources management model on the lower basin of the Diyala river, Iraq. *AIP Conf. Proc*. 3091, 020014. https://doi.org/10.1063/5.0205417

[29] S.M. Hocaoglu, M.D. Celebi, I. Basturk, R. Partal, (2021) Treatment-based hospital wastewater characterization and fractionation of pollutants, *J. Water Proc. Eng.* 43;102205.

[30] Alsultani, R., Karim, I. R., & Khassaf, S. I. (2023). Dynamic Response Analysis of Coastal Piled Bridge Pier Subjected to Current, Wave and Earthquake Actions with Different Structure Orientations. *International Journal of Concrete Structures and Materials*, 17(1), 1-15.

[31] Salahaldain, Z., Naimi, S. and Alsultani, R., (2023). Estimation and Analysis of Building Costs Using Artificial Intelligence Support Vector Machine. *Mathematical Modelling of Engineering Problems.* 10(2), pp. 405-411.

[32] S. Santana-viera, M. Esther, T. Padr_on, Z. Sosa-ferrera, J.J. Santana-rodríguez, (2020) Quantification of cytostatic platinum compounds in wastewater by inductively coupled plasma mass spectrometry after ion exchange extraction, *Microchem.* J. 157;104862.

[33] S. Mahesh, K.K. Garg, V.C. Srivastava, I.M. Mishra, B. Prasad, I.D. Mall, (2016) Continuous electrocoagulation treatment of pulp and paper mill wastewater: operating cost and sludge study, RSC Adv. 6;16223–16233.

[34] J. Liu, G. Zhu, P. Wan, Z. Ying, B. Ren, P. Zhang, Z. Wang, (2017) Current applications of electrocoagulation in water treatment: a review, Desalination Water Treat. 74; 53–70.

[35] Alsultani, R., Karim, I. R., & Khassaf, S. I. (2022) b. Dynamic Response of Deepwater Pile Foundation Bridge Piers under Current-wave and Earthquake Excitation. *Engineering and Technology Journal*, *40*(11), 1589-1604.

[36] Thair, J. M., Imad, A. D., & Riyadh, A. A. 2018. Experimental determination and numerical validation of the chloride penetration in cracked hydraulic concrete structures exposed to severe marine environment. *In IOP Conference Series: Materials Science and Engineering* (Vol. 454, No. 1, p. 012099). IOP Publishing.

[37] M. Sahul (2016), An Experimental Investigation on Treatment of Tannery Wastewater by Electro Coagulation Method.

[38] F. Kamar, K. Esgair, B. Abod, A. Nechifor *(*2018), Removal of Hexavalent Chromium Ions from the Simulated Wastewater Using Electrocoagulation Process, , pp. 111–118.

[39] R. Singh, S. Naranji, R. Husk, (2019)Recycling of Agricultural Waste for Wastewater Treatment, *Elsevier Ltd*.

[40] A. Muhmood, J. Lu, R. Dong, S. Wu, (2019) Formation of struvite from agricultural wastewaters and its reuse on farmlands : status and hindrances to closing the nutrient loop, *J. Environ. Manag.* 230; 1–13.

[41] D. Syam Babu, T.S. Anantha Singh, P.V. Nidheesh, M. Suresh Kumar, (2019) Industrial wastewater treatment by EC process, *Separ. Sci. Technol.* 1–33.

[42] Alfatlawi, T. J. M., & Alsultani, R. A. A. (2019). Characterization of chloride penetration in hydraulic concrete structures exposed to different heads of seawater: Using hydraulic pressure tank. *Engineering Science and Technology, an International Journal*, 22(3), 939-946.

[43] Mohammed, S., Shamkhi. (2022). Assessment of Manning coefficient for Dujila Canal, Wasit/-Iraq. *Open Engineering,* 13(1) doi: 10.1515/eng-2022-0388.

[44] Al-Jalili, S. K., Zwain, H. M., & Hayder, A. (2024). Generating Rainfall IDF Curves Using IMD Reduction Formula and Choosing the Best Distribution for Babylon City, Iraq. *Engineering Reports*. https://doi.org/10.1002/eng2.13053

[45] Al-Jalili, S. K., Zwain, H. M., & Hayder, A. (2024). Generating Rainfall IDF Curves Using IMD Reduction Formula and Choosing the Best Distribution for Babylon City, Iraq. *Engineering Reports*. https://doi.org/10.1002/eng2.13053

[46] Al-Khalaf, S. K., Naje, A. S., Al-Ridah, Z. A., & Zwain, H. M. (2022). Environmental Modelling of Ionic Mass Transfer Coefficient in a Unique Electrocoagulation Reactor. *Nature Environment and Pollution Technology*, *21*(4), 1587–1597. https://doi.org/10.46488/nept.2022.v21i04.011

[47] P. Rathika, S. Yamunadevi, P. Ponni, V. Parthipan, & P. Anju. (2024). Developing an AI-Powered Interactive Virtual Tutor for Enhanced Learning Experiences. *International Journal of Computational and Experimental Science and Engineering,* 10(4). https://doi.org/10.22399/ijcesen.782

[48] Olola, T. M., & Olatunde, T. I. (2025). Artificial Intelligence in Financial and Supply Chain Optimization: Predictive Analytics for Business Growth and Market Stability in The USA. *International Journal of Applied Sciences and Radiation Research,* 2(1). https://doi.org/10.22399/ijasrar.18

[49] Nuthakki, praveena, & Pavankumar T. (2024). Comparative Assessment of Machine Learning Algorithms for Effective Diabetes Prediction and Care. *International Journal of Computational and Experimental Science and Engineering,* 10(4). https://doi.org/10.22399/ijcesen.606

[50] Ibeh, C. V., & Adegbola, A. (2025). AI and Machine Learning for Sustainable Energy: Predictive Modelling, Optimization and Socioeconomic Impact In The USA. *International Journal of Applied Sciences and Radiation Research,* 2(1). https://doi.org/10.22399/ijasrar.19

[51] Duvvur, V. (2025). Modernizing Government IT Systems: A Case Study on Enhancing Operational Efficiency and Data Integrity. *International Journal of Computational and Experimental Science and Engineering,* 11(1). https://doi.org/10.22399/ijcesen.1193

[52] J. Prakash, R. Swathiramya, G. Balambigai, R. Menaha, & J.S. Abhirami. (2024). AI-Driven Real-Time Feedback System for Enhanced Student Support: Leveraging Sentiment Analysis and Machine Learning Algorithms. *International Journal of Computational and Experimental Science and Engineering*, 10(4). https://doi.org/10.22399/ijcesen.780

[53] Fowowe, O. O., & Agboluaje, R. (2025). Leveraging Predictive Analytics for Customer Churn: A Cross-Industry Approach in the US Market. *International Journal of Applied Sciences and Radiation Research ,* 2(1). https://doi.org/10.22399/ijasrar.20

[54] V. Saravanan, Tripathi, K., K. N. S. K. Santhosh, Naveenkumar P., P. Vidyasri, & Bharathi Ramesh Kumar. (2025). AI-Driven Cybersecurity: Enhancing Threat Detection and Mitigation with Deep Learning. *International Journal of Computational and Experimental Science and Engineering,* 11(2). https://doi.org/10.22399/ijcesen.1358

[55] García, R., Carlos Garzon, & Juan Estrella. (2025). Generative Artificial Intelligence to Optimize Lifting Lugs: Weight Reduction and Sustainability in AISI 304 Steel. *International Journal of Applied Sciences and Radiation Research,* 2(1). https://doi.org/10.22399/ijasrar.22

[56] G. Prabaharan, S. Vidhya, T. Chithrakumar, K. Sika, & M.Balakrishnan. (2025). AI-Driven Computational Frameworks: Advancing Edge Intelligence and Smart Systems. *International Journal of Computational and Experimental Science and Engineering,* 11(1). https://doi.org/10.22399/ijcesen.1165

[57] Hafez, I. Y., & El-Mageed, A. A. A. (2025). Enhancing Digital Finance Security: AI-Based Approaches for Credit Card and Cryptocurrency Fraud Detection. *International Journal of Applied Sciences and Radiation Research*, 2(1). https://doi.org/10.22399/ijasrar.21